Towards “Green” Smart Materials for Force and Strain Sensors: The Case of Polyaniline

Cristina Della Pina[1, a], Emanuele Zappa[2,b], Giorgio Busca[2,c], Pedro Costa[3,d], Senentxu Lanceros-Mendéz,[3,e], Annalisa Sironi[1,f] and Ermelinda Falletta[1,g]

[1] Dipartimento di Chimica, CNR-ISTM, Università degli Studi di Milano, via Golgi, 19, 20133, Milan, Italy

[2] Dipartimento di Meccanica, Politecnico di Milano, via La Masa, 1, 20158, Milan, Italy

[3] Centro/Dept. de Física da Universidade do Minho, 4710-058 Braga, Portugal

[a]cristina.dellapina@unimi.it, [b]emanuele.zappa@polimi.it, [c]giorgio.busca@polimi.it, [d]pedrofrcosta@gmail.com, [e]lanceros@fisica.uniminho.pt, [f]syron74@gmail.com, [g]ermelinda.falletta@unimi.it

Keywords: polyaniline, green synthesis, piezoresistivity, sensors.

Abstract. Stress/strain sensors constitute a class of devices with a global ever-growing market thanks to their use in many fields of modern life. As an alternative to the traditional compounds, that exhibit low inherent resistivity and limited flexibility, in the present work we will show the advantages to employ a smart material, polyaniline (PANI), prepared by an innovative green route, for force/strain sensor applications, wherein simple processing, environmental friendliness and sensitivity are particularly required.

1. Introduction

In the fabrication of commercial strain gauges the possibility to substitute metal films, characterized by low resistivity and low flexibility, with light, flexible and cheap materials is increasingly needed. In this contest, conducting organic polymers (COPs) represent an interesting alternative to traditional materials. Among them, polyaniline (PANI, Fig. 1) is particularly interesting for many aspects related to its chemical-physical characteristics: ease of synthesis, low cost, high environmental stability and unique doping/dedoping process.

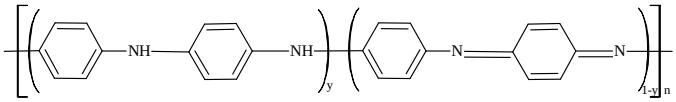

Figure 1: General structure of polyaniline.

It exists in three main forms, that differ from the oxidation grade, ranging from the totally reduced leucoemeraldine (y = 1) to the half-oxidized emeraldine (y = 0.5) as well as the totally oxidized pernigraniline (y = 0). Only the half-oxidized and half-protonated form, emeraldine salt (ES), exhibits electroconductive properties and for this reason it has received large attention.
However, there are not enough information on the piezoresistivity of pristine polyaniline. Only two works were published [1], bringing different results. In fact, on the one hand Lillemose *et al*. reported negative GF (gauge factor) values of about -5 in 4-point bending experiments, whereas on the other hand the GFs obtained by Lanceros-Méndez and co-workers ranged from 10 to 22. All these results were obtained using commercial polyaniline (PANIPOL®T) [2], prepared by a traditional approach, based on aniline monomer polymerization. As an alternative to traditional PANI synthesis, that employ “stoichiometric oxidants” [3] leading the formation of many polluting and/or carcinogenic co-products, we recently addressed our efforts on developing new green methods for the COPs preparation [4], obtaining PANI characterized by high solubility and purity. Herein, we will report the preparation and characterization of “green” PANI and its electromechanical response as pellet [5] and film.

2. Experimental Procedure

2.1. Synthesis of "Green" Polyaniline

2 g of *N*-(4-aminophenyl)aniline (aniline dimer, AD) were dissolved in 27 mL of HCl 0.4 M (AD/HCl= 1, molar ratio) at room temperature. Then, 5.60 mL of H_2O_2 30% (H_2O_2/AD= 5, molar ratio) were quickly added, immediately followed by 0.54 mL of Cu^{2+} 0.02 M aqueous solution (AD/Cu^{2+}= 1000, molar ratio). An insoluble green powder was collected after 24 hours by filtration, washed several times by water and acetone and dried under air. 1 g of this product, (yield of 73%) spectroscopically identified as emeraldine salt, was deprotonated by stirring in 20 mL of NH_4OH 0.5 M at room temperature. After 24 hours, a dark blue product (emeraldine base, EB) was filtered, washed several times with water until the mother liquors became neutral and dried under air.

2.2. PANI/H_2SO_4 Pellet Preparation

500 mg of EB were reprotonated by 9 mL of H_2SO_4 0.3 M (AD/H_2SO_4= 1, molar ratio), thus obtaining PANI/H_2SO_4. After 6 hours, the dark green product was filtered, washed several times with water and dried under air. H_2SO_4 was chosen as the doping agent for its chemical and thermal stability. Two pellets having diameter of 13 mm and thickness of 1 mm were prepared pressing 200 mg of PANI/H_2SO_4 for 30 minutes at 100 kN using an Atlas Manual Hydraulic Press.

2.3. PANI/CSA Film Preparation

500 mg of EB were dispersed in 20 mL of $CHCl_3$. Then, 631 mg of camphorsulfonic acid (CSA, AD/CSA= 1, molar ratio) were added into the solution and stirred at room temperature. After 24 hours, a green solution containing soluble PANI/CSA was separated by the insoluble part by filtration and then evaporated under vacuum (solubility of PANI/CSA in chloroform is 13 mg/mL).
10 mL of this PANI/CSA solution were deposited by drop casting on polyethylene terephthalate (PET) substrates and solvent was evaporated under air.

2.4. Samples Characterization

FT-IR spectra were recorded on a JASCO FT/IR-410 spectrophotometer in the 500-4000 cm^{-1} range. UV-vis spectra were recorded on a Hewlett Packard 8453 spectrophotometer using *N*,*N*-dimethylformamide and chloroform as the solvent. XRD analyses were performed using a Rigaku D IIIMAX horizontal-scan powder diffractometer with Cu Kα radiation.
PANI-based pellets uniaxial compression tests were carried out with a MTS alliance RT/100 universal mechanical test machine. The axial displacements were measured by a deflectometer MTS model 632.06H-30. In order to carry out these tests, PANI/H_2SO_4 samples were sandwiched between two circular copper plates connected to a multimeter and placed between two steel disks, isolated with respect to the loading machine by means of thin non-conductive films. The PANI pellet support ensures at the same time a homogeneous distribution of loads on the pellet surface and the electrical resistance measurement by the connection with the multimeter. After a first stabilization cycle carried out on the support in the absence of any sample, for each pellet three loading/unloading cycles were performed in a range of 0 kN-100kN with a loading step of 10kN.
In the case of PANI/CSA films two parallel rectangular gold electrodes were deposited by magnetron sputtering on one side of the sample and two copper wires were attached to the electrodes to ensure good electrical contact. PANI/CSA electromechanical properties were investigated by 4-point-bending tests in a Shimadzu-AG-IS 500 N testing instrument at a speed of 2.5 mm/min and a maximum vertical (z axis) displacement of 2.5 mm while simultaneously measuring the electrical resistivity variation with a digital multimeter Agilent 34401A.
The electrical conductivity values were estimated indirectly from resistivity (ρ) determination from the I-V curves measurements performed in direct current (DC) mode with an applied voltage ranging between ± 5V, at room temperature with a Keithley 487 picoammeter/ voltage source. The resistivity was calculated from Equation: $\rho = R \cdot (A/\ell)$, where R, A and ℓ are the electrical resistance (Ohm), the cross-sectional area (m^2) and the length (m) of the piece of material respectively.

3. Results and Discussion

3.1. "Green" Polyaniline Advantages

The most common polyaniline synthesis is based on the radical oxidative polymerization of aniline monomer. Wei *et al*. demonstrated that the aniline monomer oxidation to form dimeric species [*N*-(4-aminophenyl)aniline, *trans*-azobenzene and benzidine] is the thermodynamic limitation of the process [6]. Once dimers are produced, they react immediately leading to first oligomers and then polymers.If on the one hand the *trans*-azobenzene formation can affect the structure, purity and conductivity of PANI, on the other hand the benzidine production is risky for its toxic and carcinogenic properties [7], limiting the potential application of PANI produced by this way, in particular in the medical and biomedical sectors. On the contrary, the oxidative polymerization of *N*-(4-aminophenyl)aniline does not result in benzidine formation [8]. Moreover, this approach leads to a kind of PANI characterized by relatively short chains (low molecular weights) [9] that increase the polymer processability (e.g., solubility [10]) but at the same time reduces its conductivity [6c, 9]. The use of *N*-(4-aminophenyl)aniline as the reagent overcomes the thermodynamic limitation discussed above, allowing to carry out the reaction by the use of milder oxidant, such as molecular oxygen and hydrogen peroxide in the presence of specific catalysts[5c-d, 10].

3.2. Spectroscopic Characterization

The FT-IR and UV-vis spectra (Fig. 2A, C and D) show that both (PANI/H_2SO_4 and PANI/CSA) were obtained in the form of conductive emeraldine salt.

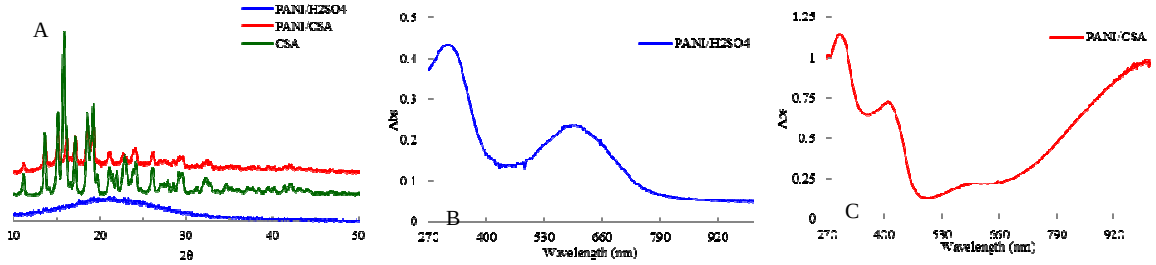

Figure 2: A) XRPD patterns of both PANI/H_2SO_4 and PANI/CSA, B) UV-vis spectrum of PANI/H_2SO_4 in dimethylformamide, C) UV-vis spectrum of PANI/CSA in chloroform.

FT-IR spectra (Data not shown) show the typical C=C stretching bands of the quinoid (N=Q=N) and benzenoid rings (N-B-N) at 1570 cm^{-1} and 1498 cm^{-1}, respectively. When the ratio between these two bands is around one, as in this case, polyaniline is in form of emeraldine, because this means that it contains a similar number of benzenoid and quinoid rings [11]. Owing to the different solubility of PANI, related to the different doping agents employed, UV-vis spectra were recorded in different solvents. The UV-vis spectrum reported in Fig. 2B is typical of emeradine base [12]. In fact, dimethylformamide is able to dedop the polymer in solution [13]. The bands at 311 and 603 nm are respectively related to the π–π^* transition of the benzenoid rings and the HOMO-LUMO transition, that is a benzenoid to quinoid excitonic transition. On the contrary, the UV-vis spectrum of PANI/CSA (Fig. 2C) shows the characteristic bands of PANI in form of conducting emeraldine salt. Two new bands appear at 402 and 990 nm, assigned to the polarons and bipolarons formation respectively. The latter band, typically observed at lower wavelengths (790-856 nm) [14], is shifted in the visible region. This bathochromic effect can be attributed to materials nanostructured form, π conjugation extension [15], but more probably change of polymeric chains conformation in solution from coil-like to rod-like [16]. Finally, XRPD patterns emphasize the different crystallinity degree of both materials. Low PANI crystallinity can be related to different factors: conditions of synthesis, kind and amount of acid used as the doping agent, molecular weight and random orientation of polymeric chains [17]. As shown in Fig. 2A, the XRPD pattern of PANI/H_2SO_4 is characteristic of an amorphous material with a broad band at $2\theta \approx 20$ [18]. On the contrary, PANI/CSA sample

exhibits higher crystallinity strictly related to the presence of a crystalline dopant. However, also in this case the broad band of PANI is evident.

3.3. Electrical conductivity

Concerning electrical conductivity, PANI/H_2SO_4 ($7.62 \cdot 10^{-6}$ S/cm) is about 45 times more conductive than PANI/CSA ($1.67 \cdot 10^{-7}$ S/cm). PANI conductivity is affected by many parameters: amount and kind of dopant [19], humidity [20], degree of crystallinity [21] and molecular weight [22, 23]. Concerning the type of dopant employed, a key role is played by its dimensions. Regarding this aspect, it is to notice that the polyaniline conductivity is the sum of two contributions: the ability of the charge carriers to move along the polymer backbone by an *intra*-chain conduction mechanism and their ability to hop between neighbouring polymeric chains by an *inter*-chain conduction mechanism. This second contribution becomes particularly important when the material is subjected to a deformation. The *inter*-chain distance is strongly dependent on the dopant size, kind of polymeric backbone-dopant interactions (typically hydrogen bonds) and structural rigidity [24]. In our case the steric hindrance of camphorsulfonic acid is much greater than that of sulphuric acid, limiting the carrier movement between chains and, therefore, decreasing the polymer conductivity. Moreover, the pellets were prepared by pressing the overall PANI/H_2SO_4 sample, whereas for the films preparation only the portion of PANI/CSA sample soluble in CH_3Cl, containing shorted polymeric chains. For this reason, even though samples were not characterized in terms of molecular weights, it is possible to conclude that PANI/CSA sample consists on polymeric chains shorter than those of PANI/H_2SO_4 sample.

3.4. Electromechanical Response

3.4.1. PANI/H_2SO_4 Pellet

As recently demonstrated [5], after an initial mechanical material stabilization during the first force–compression cycle, the subsequent ones are almost linear and hysteresis-free (Fig. 3A), even though two different regimes can be recognized: below and over ~0.1 mm in 1mm tick pellet.

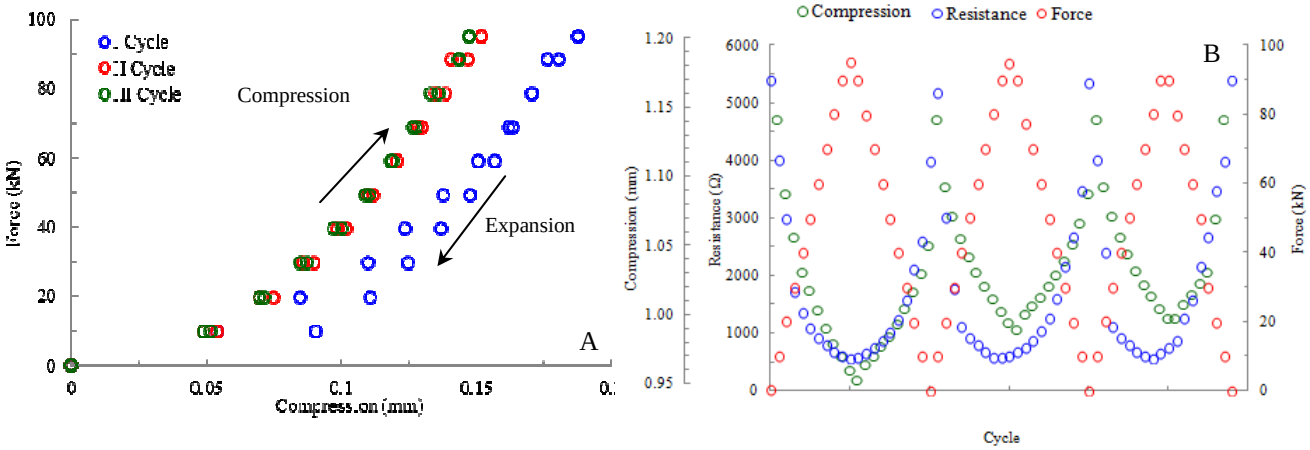

Figure 3: A) Force vs compression curves and comparison between B) Resistance, Force and Compression variation under compression/expansion cycles.

These two regimes can be attributed to the presence of voids among the polymeric chains, which can be reduced by the application of high loads. The electrical resistance of the sample decreases upon loading and increases upon unloading reversibly and almost linearly. A resistance variation of about 87% is observed in the range of 0-100 kN (Fig. 3B), corresponding to a compression range of 0-17% (Fig. 3B). However, the GF value of the PANI/H_2SO_4 pellets is < 1. In this case, PANI works as a metal, whose change in resistance is mainly due to geometrical factors (see Eq. 1) [25]. The low GF can be correlated to the low degree of crystallinity of the material. In fact, this latter indicates a random orientation of the polymeric chains in the pellet that can reduce or even suppress the contribution of *inter*-chain mechanism to the overall conductivity of the sample. In this context,

the use of a dopant with high steric hindrance and the possibility to process the polymer as films should emphasize the piezoresistivity of the material. For this H_2SO_4 was replaced with CSA..

3.4.2. PANI/CSA Film

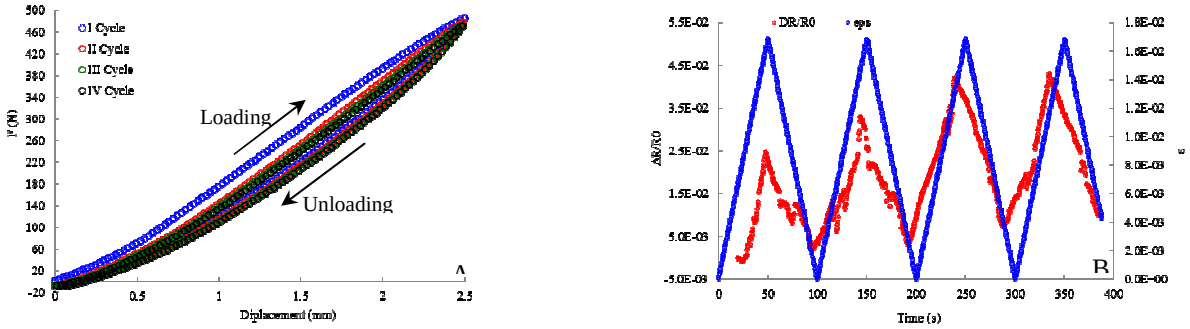

Figure 4: A) Force-displacement curves and B) cyclic piezoresistive response as a function of time for PANI/CSA.

It is observed that during the first cycle the mechanical hysteresis is particularly evident and increases with increasing deformation. However, it becomes less evident with increasing the number of cycles. Also in this case, it is possible to recognize two regimes: below and above ~ 0.6 mm. The first zone shows a nonlinear and almost hysteresis free trend, whereas in the second region a more linear profile characterized by larger hysteresis appears. In order to explain the presence of two regimes, it is possible to hypothesize two different types of polymer reconfigurations: a morphological modification at low loads and a molecular one at higher loads. Figure 4B shows that electrical resistance changes almost linearly and reversibly with the applied strain, even though it exhibits a growing trend, probably due to a mechanical instability of the material. The GF values, evaluated by the slope of the linear fit between $\Delta R/R_0$ and ε, are in agreement with those of the PANI/H_2SO_4 pellet. However, they increase linearly with increasing the number of cycles, suggesting a mechanical instability of the material, according to the results obtained by in stress–strain tests (Fig. 4A). These results can be attributed to the irregular morphology and high porosity of the material, as confirmed by SEM (Data not shown). Further investigations are in progress to improve the polymer performance.

Acknowledgements

This work was supported by FEDER through the COMPETE Program and by the Portuguese Foundation for Science and Technology (FCT) in the framework of the Strategic Project PEST-C/FIS/UI607/2011 and the project Matepro –Optimizing Materials and Processes", ref. NORTE-07-0124-FEDER-000037", co-funded by the "Programa Operacional Regional do Norte" (ON.2 – O Novo Norte), under the "Quadro de Referência Estratégico Nacional" (QREN), through the "Fundo Europeu de Desenvolvimento Regional" (FEDER). The authors also thank FCT for financial support under project PTDC/CTM-NAN/112574/2009. The authors also thank the COST Actions MP1003 (European Scientific Network for Artificial Muscles, ESNAM) and MP0902 (Composites of Inorganic Nanotubes and Polymers, COINAPO).

References

[1] M. Lillemose, M. Spieser, N.O. Christiansen, A. Christiansen and A. Boisen: Microelectron. Eng. 85 (2008) p. 969; J. Nunes Pereira, P. Vieira, A. Ferreira, A.J. Paleo, J G. Rocha and S. Lanceros-Méndez: J. Polym. Res. 19 (2012) p. 9815

[2] http://www.scmchem.com/eWebEditor/UploadFile/2006711164022504.pdf

[3] G.G. Wallace, G.M. Spinks, L.A.P. Kane-Maguire and P.R. Teasdale in: Conductive Electroactive Polymers: Intelligent Polymer System0s (CRC Press, London, 2009)

[4] a) Z. Chen, C. Della Pina, E. Falletta, M. Lo Faro, M. Pasta, M. Rossi and N. Santo: J. Catal. 259 (2008) p. 1; b)C. Della Pina, E. Falletta, M. Lo Faro, M. Pasta and M. Rossi: Gold Bull. 42-1 (2009) p. 27; c) Z. Chen, C. Della Pina, E. Falletta and M. Rossi: J. Catal. 267 (2009) p. 93; d) C. Della Pina, E. Falletta and M. Rossi: Cat. Today 160 (2011) p. 11; e)C. Della Pina, M. Rossi, A.M. Ferretti, A. Ponti, M. Lo Faro and E. Falletta: Synth. Met. 162 (2012) p. 2250

[5] C. Della Pina, E. Zappa, G. Busca, A. Sironi and E. Falletta: Sensor. Actuat. B-Chem 201 (2014) p. 395-401

[6] a) Y. Wei, G.-W. Jang, Ch.-Ch. Chan, K.F. Hsuen, R. Hariharan, S.A, Patel and C.K. Whitecar: J. Phys. Chem. 94 (1990) p. 7716; b) Y. Wei, X. Tang, Y. Sun and W.W. Focke: J. Polym. Sci. 27 (1989) p. 207

[7] M. H. –C. Chen, L. –C. Hsu, J. –L. Wu, C. -W. Yeh, J. –N. Tsai, Y. –C. Hseu and L. –S. Hsu:

Environ. Toxic. (2013) p. 1-9

[8] E. M. Geniès, J. F. Penneau, M. Lapkowski and A. Boyle: J. Electroanal. Chem. 269 (1989) p. 63-75

[9] A. Kitani, J. Yano, A. Kunai, K. Sasaki: J. Electroanol. Chem. 221 (1987) 69-82

[10] P. Frontera, C. Busacca, S. Trocino, P. Antonucci, M. Lo Faro, E. Falletta, C. Della Pina and

M. Rossi: J. Nanosci. Nanotechno. 13 (2013) p. 4744-4751

[11] X. Feng, C. Mao, G. Yang, W. Hou and J. Zhu: Langmuir 22 (2006) p. 4384-4389

[12] K. Mallick, M. J. Witcomb, A. Dinsmore and M. S. Scurrell: J. Polym. Res. 13 (2006) p. 397-401

[13] Y. H. Geng, Z. C. Sun, J. Li, X. B. Jing, X. H. Wang and F. S. Wang: Polymer 40 (1999) p.

5723-5727

[14] J. Stejskal and P. Kratochvil: Synth. Met. 61 (1993) p. 225-231

[15] S. E. Moulton, P. C. Innis, L. A. P. Kane-Maguire, O. Ngamna and G. G. Wallace: Curr. Appl. Phys. 4 (2004) p. 402–406

[16] J. Laska: J. Mol. Stuct. 701 (2004) p. 13-18

[17] M. Pyo and J. -H. Hwang: Synth. Met. 159 (2009) p. 700-704

[18] M. Sivakumar and A. Gedanken: Synth. Met. 148 (2005) 301-306

[19] M. D. Catedral, A. K. G. Tapia, R. V. Sarmago, J. P. Tamayo and E. J. Del Rosario: Science Diliman, 16 (2004) p. 41-46

[20] Q. Zhou, J. Wang, Y. Ma, C. Cong and F. Wang: Colloid. Polym. Sci. 285 (2007) p. 405-411

[21] S. Bhadra, N. K. Singha and D. Khastgir: Synth. Met. 56 (2006) p. 1148-1154

[22] S. Bhadra, S. Chattopadhyay, N. K. Singha and D. Khastgir: J. Polym. Sci., Part B: Polym. Phys. 45 (2007) p. 246-259

[23] R. Pelster, G. Nimtz and B. Weissling: Phys. Rev. B 49 (1994) p. 12718-12723

[24] J. Joo, H. G. Song, Y. C. Chung, J. S. Baeck, S. K. Jeong, J. S. Suh and E. J. Oh: J. Korean. Phys. Soc. 30 (1997) p. 230-236

[25] E. Defaÿ, C. Millon, C. Malhaire and D. Barbier: Sensor. Actuat. A-Phys. 33 (1992) 53-56